

DIURNAL MAPPING OF $[H_2O]$, $[HDO]$, $[HDO]/[H_2O]$, AND $O_2(a^1\Delta_g)$ EMISSION ON MARS USING GROUND BASED HIGH-RESOLUTION SPECTROSCOPY

R.E. Novak, Iona College, New Rochelle NY USA, (rnovak@iona.edu), **M. J. Mumma**, **G. L. Villanueva**, NASA-Goddard Space Flight Center, Greenbelt, MD, USA

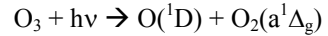
Introduction:

We report recent investigations of HDO, H_2O , and $O_2(a^1\Delta_g)$ emission (a tracer for ozone above 20 km) on Mars for data taken on 3 April 2010 ($L_s = 72.5^\circ$). CSHELL on the NASA-IRTF was used for our observations. The slit was positioned E/W on Mars centered at the sub-Earth point ($14^\circ N$, Fig. 1A). Data at HDO, H_2O , and $O_2(a^1\Delta_g)$ emission settings were taken over a four-hour period in UT. This is part of a larger study to measure the seasonal and geographical variation of HDO, H_2O , their ratio, and the $O_2(a^1\Delta_g)$ emission. These results may be used to obtain better insights into the dynamics of Mars' atmosphere. We have previously presented latitudinal maps for several seasonal dates [1-7]. We now present longitudinal/diurnal maps.

The preferential escape of the lighter hydrogen isotope controls the global $[HDO]/[H_2O]$ abundance ratio [8]. A comparison of the present abundance levels with escape models provides an estimate of the amount of water lost over time. Furthermore, Mars water undergoes seasonal cycling and (perhaps) bulk fractionation in polar ice or even aerosols.

Our group has conducted observing programs to measure the $[HDO]/[H_2O]$ ratio and the $O_2(a^1\Delta_g)$ emission rate for different seasons and positions on Mars. DiSanti and Mumma [9] developed a technique for mapping HDO on Mars through its v_1 fundamental band near $3.67 \mu m$ using CSHELL at the NASA-IRTF. Novak [1] extended the approach significantly and measured the $O_2(a^1\Delta_g)$ emission rate and the column density of HDO on Mars for data acquired in January 1997. For data taken from 1997 to 2003, we compared our HDO data to H_2O results obtained from TES [10]. Since 2003, we have been using absorption lines near $3.33 \mu m$ (the $2v_2$ band) to determine H_2O abundances. With long slit spectrometers, we now map the two species using the same spectrometer-telescope combination, eliminating many sources of systematic error. Our observations have shown variations in the $[HDO]/[H_2O]$ ratio [2,5,6].

Ozone in Mars' atmosphere is photolyzed by absorption of UV light (Hartley band, 220-320 nm) from the sun. There are two primary routes for the products. The following has a quantum yield of 0.9:



The $O_2(a^1\Delta_g)$ state decays radiatively through magnetic dipole transitions with a lifetime $\tau \sim 3800$ s [11]. The state is also quenched by collisions with CO_2 . Collisional quenching dominates at altitudes less than 20 km. Measurements of the $O_2(a^1\Delta_g)$ emis-

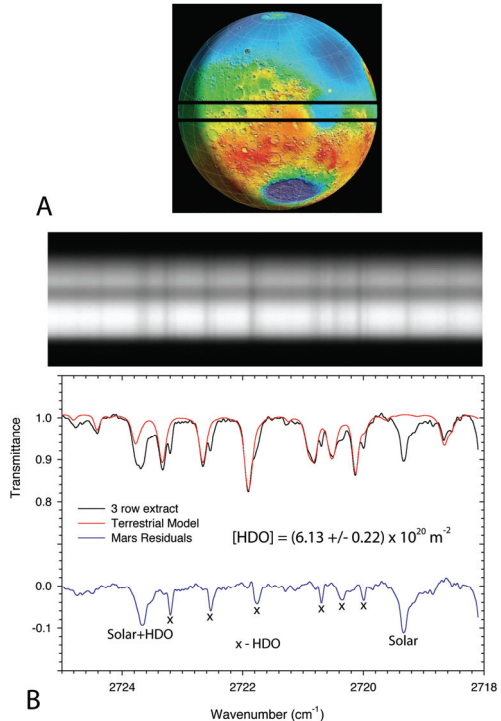


Figure 1: **A.** Position of the slit across Mars on 3 Apr 2010, 7:29 UT [14]. The image of the sub-Earth position was centered within the spectrograph slit. **B.** Spectral-spatial image at HDO setting. Three-row extract is centered at $327^\circ W$, $14^\circ N$. The Martian HDO lines are red shifted with respect to the terrestrial lines. A terrestrial atmospheric model (red) is subtracted from the observed trace yielding the Martian absorption lines (bottom). The best-fit of this trace by Mars atmospheric models yields the column density of HDO.

sion are thus used to determine the ozone column abundance above 20 km. [1]

[HDO], $[H_2O]$ Observations: We have reported our results and methods for obtaining and analyzing

column densities of H₂O, HDO, and the corresponding [HDO]/[H₂O] ratio. A detailed description of

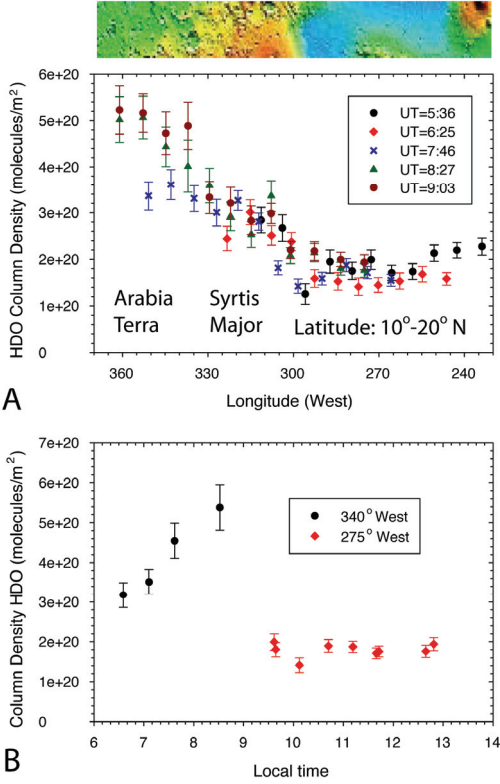


Figure 2: **A.** Retrieved HDO column densities over a four-hour period. The cropped Mars-MOLA map indicates the location of the retrieve points. **B.** Retrieved data points centered at 275° and 340° adjusted to local time.

our data acquisition and analysis routines was recently published [6]. Here, we present longitudinal/diurnal maps for [HDO] and [H₂O] values taken on 03 April 2010 ($L_s = 72.5$, Fig. 1). The slit was positioned E/W on Mars centered at 14°N latitude. Observations at HDO, H₂O, and O₂(a¹Δ_g) emission settings were repeatedly taken over a four-hour period in UT.

Maps for [HDO] versus longitude are presented in Fig. 2A. For two locations (275°W and 340°W, Fig. 2B), the column density is plotted versus local time. The results at 275°W were accumulated over local times 9:00-13:00; the surface elevation for this region is ~ -3.5 km. The measured column densities are constant during. On the other hand, column densities of HDO at 340°W increase between 6:30 and 9:00 LT. The elevation for this region (~ -0.5 km) is higher than at 275°W. This increase is interpreted as being cause by the vaporization of frost and water-ice clouds after sunrise. The frost and water-ice clouds are formed during the night. Clouds have a tendency to form over highland regions rather than

lowlands [12], resulting in greater values and variation at 340°W than at 275°W.

Longitudinal maps of [HDO] and [H₂O] surrounding 14°N are presented in Fig. 3 along with their ratio. The column densities of both species and their ratio are greater in the highland region. The water-ice formations have a tendency to accumulate [HDO] rather than [H₂O].

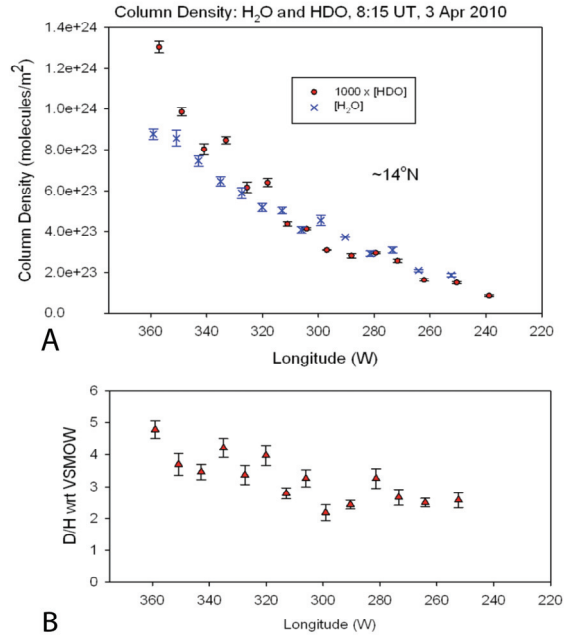


Figure 3: **A.** Column densities of HDO and H₂O at 8:15 UT, 3 April 2010. The slit was positioned E/W on Mars centered at 14°N. **B.** Using the values in Fig. 3A, the ratio between [HDO] and [H₂O] on Mars compared to the Vienna Standard Ocean Mean Water (VSMOW) on Earth.

O₂(a¹Δ_g) Emission Observations: We have been observing the O₂(a¹Δ_g) emission on Mars since 1997 [1]. From our measurements, we derived the column

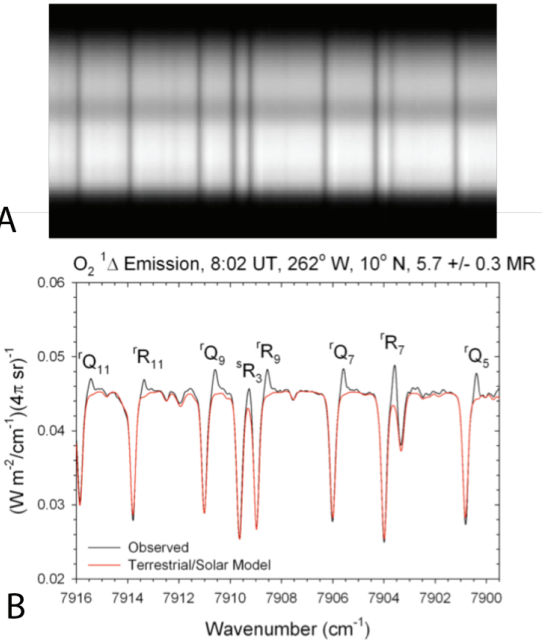


Figure 4: **A.** spectral-spatial image centered at 7908 cm⁻¹ taken 3 April 2010. **B.** Three row extract from Fig. 4A. Black curve is the observed spectrum; red curve is the terrestrial model. The labeled emissions are Doppler shifted from their terrestrial absorptions.

abundance of ozone above 20 km. A spatial/spectral image at an $O_2(a^1\Delta_g)$ emission setting is given in Fig. 4A; a three row extract that shows the emission lines is given in Fig. 4B. From measuring the areas of the Mars emission lines, we determine the rotational temperature of the $O_2(a^1\Delta_g)$ state and from that, the total emission rate.

Vertical emission rates taken over a four-hour time span are shown in Fig. 5. The rates are plotted versus local time. They show a similar growth in intensity between sunrise and mid-day regardless of surface altitude. During this season, Mars is near aphelion and the hygropause is low in altitude (~ 10 km). The $O_2(a^1\Delta_g)$ emission extends across the planet. Our results show a strong variation with respect to local time.

Conclusion and Future Plans:

We presented longitudinal/diurnal maps of [HDO], $[H_2O]$, their ratio, and the $O_2(a^1\Delta_g)$ emission for $L_s = 72.5^\circ$. Using updated analysis tools [6], we intend to further analyze archival data. We have telescope time scheduled for $L_s = 78.5^\circ$ (19-20 Jan 2014). We intend to repeat the measurements at local times of 10:00 – sunset, thus complementing the

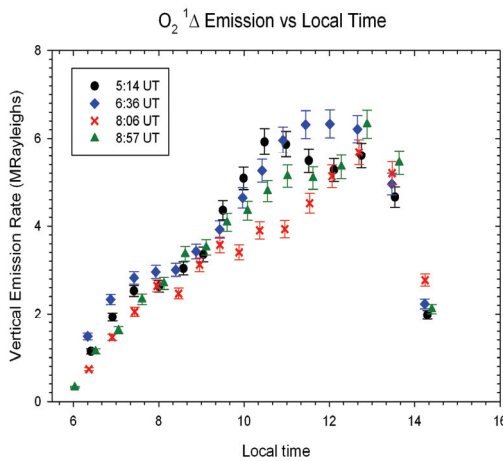


Figure 5: Vertical column $O_2(a^1\Delta_g)$ emission rates taken at four times. Emission rates are obtained from extracts as in Fig. 4., and are plotted as a function of local time on Mars. Rates show similar increases during morning hours and peak near 12:00. Future observations are planned to obtain emission-rates during afternoon hours.

results presented here (Fig 3 and Fig. 5). We have also proposed telescope time for $L_s \sim 90^\circ$ and $L_s \sim 146^\circ$. We plan to continue our observations during future Mars apparitions and to use ISHELL [13] which is currently being constructed at the NASA-IRTF. ISHELL is a cross-dispersed IR-spectrograph that can measure both HDO and H_2O bands simulta-

neously with a better sensitivity than CSHELL.

In addition to the observations described here, we plan to monitor water-ice clouds by taking CO_2 measurements at two different wavelengths (3.20 and 3.65 μm). Path lengths at these wavelengths will be compared to altitude results from MOLA. We plan to determine the diurnal variation of water-ice clouds. Our results are being used as comparison to results from Mars Curiosity [15,16]. We also plan to continue the measurement of the [HDO]/[H_2O] ratio in the future to support the MAVEN mission (Nick Schneider, private communication).

Acknowledgements:

REN was supported by NSF RUI Grant AST-0805540. MJM and GLV were supported by Grants from NASA's Planetary Astronomy Program (344-32-51-96) and Astrobiology Program (344-53-51). We acknowledge the Director and Staff of the NASA Infrared Telescope Facility for granting us observing time. The NASA-IRTF is operated by the University of Hawaii under Cooperative Agreement NNX-08AE38A with the National Aeronautics and Space Administration, Science Mission Directorate, Planetary Astronomy Program.

References:

- [1] Novak, R. et al., (2002), *Icarus*, **158**, 14-23.
- [2] Mumma, M. et al. (2003), Sixth International Conference on Mars, Abstract # 3186. [3] Novak R. et al. (2007), Seventh International Conference on Mars, Abstract # 3283. [4] Villanueva et al., (2008) Mars Atmosphere: Modelling and Observations, Abstract # 9101. [5] Fisher, D. et al. (2008), *J. Geophys. Res.*, **113**, E00A15. [6] Novak R. et al. (2011), *Planet. Space Sci.*, **59**, 163-168. [7] Novak R. et al. (2013), AAS, DPS # 45, 313.04. [8] Montmessin F. et al. (2005), *J. Geophys. Res.*, **110**, E03006. [9] DiSanti, M. and Mumma, M (1995), *Workshop on Mars Telescope Observations*, (Cornell U. Press). [10] Smith, M., (2007), *Icarus*, **167**, 148-165. [11] Badger, R.M. (1965), *J. Chem. Phys.*, **43**, 4345-4350.
- [12] Hinson, D.P. et al., (2013), AAS DPS#45, 500.04. [13] Tokunaga et al, (2008), *Proc. SPIE*, **7014**, 70146A-70146A-11. [14] Schmunk R and Allison, M. (2008), <www.giss.nasa.gov/tools/Mars24>. [15] Leshin, L.A. et al., (2013), 44th Lunar and Planetary Science Conference, No. 1719, p. 2234. [16] Webster, C. R. et al., (2013) *Science*, Vol. 341, 260-263.